Applied Catalysis B: Environmental 147 (2014) 411–419

Contents lists available at ScienceDirect

Applied Catalysis B: Environmental

journal homepage: www.elsevier.com/locate/apcatb

Effects of reducing agents on the degradation of 2,4,6-tribromophenol in a heterogeneous Fenton-like system with an iron-loaded natural zeolite

Shigeki Fukuchi, Ryo Nishimoto, Masami Fukushima *, Qianqian Zhu

Laboratory of Chemical Resources, Division of Sustainable Resources Engineering, Graduate School of Engineering, Hokkaido University, Sapporo 060-6828, Japan

ARTICLE INFO

Article history:
Received 4 February 2013
Received in revised form
17 September 2013
Accepted 20 September 2013
Available online 1 October 2013

Keywords:
Fe-loading
Natural zeolite
2,4,6-Tribromophenol
Heterogeneous Fenton system
Reducing agents

ABSTRACT

The effects of reducing agents on the degradation of 2,4,6-tribromophennol (TrBP) were investigated in a heterogeneous Fenton-like system using an iron-loaded natural zeolite (Fe-Z). The catalytic activity for TrBP oxidation in the presence of the Fe-Z and H_2O_2 was not appreciable. The addition of a reducing agent, such as ascorbic acid (ASC) or hydroxylamine (NH_2OH), resulted in an enhancement in the degradation and debromination of TrBP. TrBP was completely degraded and debrominated at pH 3 and 5 in the presence of NH_2OH, while the degradation was significantly suppressed at pH 7 and 9. Although the rates of TrBP degradation were relatively constant at pH 3, 5, 7 and 9 in the presence of ASC, the percent degradation reached a plateau at 70%. These results show that ASC functions as a strong HO• scavenger, as opposed to NH_2OH, at pH 3 and 5. Thus, adding NH_2OH is preferable for the degradation of TrBP via a Fenton-like system using Fe-Z as the catalyst. It is noteworthy that the complete mineralization of TrBP was achieved at pH 5, when NH_2OH and H_2O_2 were sequentially added to the reaction mixture. Analysis of the surface of Fe-Z by X-ray photoelectron spectrometry indicated that the Fe(III) on the surface of the catalyst was reduced to Fe(II) after treatment with ASC. Thus, the role of RAs can be of assistance in Fe(III)/Fe(II) redox cycles on the Fe-Z surface and enhance the generation of HO• via the decomposition of H_2O_2.

1. Introduction

2,4,6-Tribromophenol (TrBP) is used in the manufacturing of TVs, computers and other household electric appliances as a flame retardant intermediate. As a result of extensive use, TrBP can be found in soils, landfill leachates and sewage sludge [1]. TrBP could have an endocrine disrupting activity *in vivo*, because it has been shown to interfere with the thyroid hormone system by competitive binding to transport proteins [2]. In terms of reducing the potential for pollution and related health issues, it is important to develop the techniques for the oxidative degradation of TrBP in contaminated environments. However, bromophenols are more difficult to oxidize than other halogenated phenols, such as fluorophenols and chlorophenols [3].

Fenton and Fenton-like processes have been the focus of studies dealing with the oxidative degradation of organic pollutants. In such systems, H_2O_2 is catalytically decomposed by Fe(II) to generate a powerful oxidant, the hydroxyl radical (HO•). The overall process is referred to the Haber–Weiss reaction as below [4]:

$$Fe(II) + H_2O_2 \rightarrow Fe(III) + HO^{\bullet} + OH^{-} \quad (k = 63\,M^{-1}\,s^{-1}[5]) \tag{1}$$

Numerous studies related to the degradation of chlorophenols by homogeneous Fenton and Fenton-like systems have appeared [6–8], but much less information is available concerning the degradation of bromophenols. The homogeneous Fenton processes is limited to the pH range from 2.5 to 3.5, because Fe(III)-hydroxides are converted into sludge, leading to the deactivation of catalytic activity for oxidation [9]. To overcome such problems, heterogeneous Fenton-like systems in which Fe(II) or Fe(III) are supported to a solid support have been examined: e.g., minerals [10–13] and cation exchange resins [14,15].

In particular, Fe-loaded zeolites have been demonstrated to function as active catalysts in the degradation of organic pollutants in the presence of H_2O_2 [16–21]. In these studies, synthesized zeolites such as Y-, ZSM-5 and Beta zeolites were mainly employed and Fe^{2+} or Fe^{3+} were loaded via cation-exchange reactions. Although natural zeolites are cheap and widely distributed, they have not been used extensively as catalysts, but are mainly utilized as

* Corresponding author. Tel.: +81 11 706 6304; fax: +81 11 706 6304.
E-mail address: m-fukush@eng.hokudai.ac.jp (M. Fukushima).

0926-3373/$ – see front matter © 2013 Elsevier B.V. All rights reserved.
http://dx.doi.org/10.1016/j.apcatb.2013.09.032

Table 1
Inorganic element content, cation exchange capacity (CEC), specific surface area (SSA), total pore volume and average pore diameter for original zeolite and Fe-Z.

Sample	Inorganic elements (%)				CEC (cmol kg^{-1})	SSA (m^2 g^{-1})	Total pore volume (cm^3 g^{-1})	Average pore diameter (nm)
	Al	Si	Ca	Fe				
Original zeolite	2.5 ± 0.46	40.8 ± 5.7	21.4 ± 1.4	0.49 ± 0.05	150 ± 22	33.3	0.108	13
Fe-Z	2.38 ± 0.22	38.9 ± 0.02	14.9 ± 0.2	1.54 ± 0.06	71.7 ± 6.1	26.2	0.131	20

adsorbents [22] and soil amendments [23–25]. The surface areas of natural zeolites (16–38 m^2 g^{-1}) [22–25] are much smaller than those the synthesized materials (300–800 m^2 g^{-1}) [17–21], because of the presence of impurities such as quartz and feldspar. Such smaller surface areas of natural zeolites may be a disadvantage in terms of achieving a higher catalytic activity.

In homogeneous system, Fenton and Fenton-like systems combined with light irradiation [7,8,26] and electrochemical processes [27] have been examined to accelerate the redox cycle of Fe(III)/Fe(II) and the generated $HO^{\bullet}$. Although the addition of reducing agents (RAs) seems to be simple and effective in accelerating the reduction of Fe(III) to Fe(II), they may also serve as inhibitors of oxidative Fenton processes because of their oxidation by $HO^{\bullet}$. It has, however, been reported that the addition of RAs, such as ascorbic acid (ASC) and hydroxylamine (NH_2OH), to homogeneous Fenton-like systems can be effective in enhancing the generation of $HO^{\bullet}$, ultimately leading to the degradation of organic substrates [28–30]. In the present study, the addition of RAs, such as ASC, NH_2OH, *p*-hydroquinone, oxalic, gallic and humic acids, to a heterogeneous Fenton-like system with an iron-loaded natural zeolite (Fe-Z) was examined. The reactivity of the heterogeneous Fenton-like system was evaluated using the oxidative degradation of TrBP as a model system.

2. Materials and methods

2.1. Materials

ASC, NH_2OH, *p*-hydroquinone, oxalic and gallic acids, employed as RAs, were purchased from Nacalai Tesque (Kyoto, Japan). The humic acid, a natural RA, was extracted from a Shinshinotsu peat soil sample (Hokkaido, Japan), as described in a previous report [31]. TrBP (98% purity) was purchased from Tokyo Chemical Industry (Tokyo, Japan), and a stock solution (0.01 M) was prepared by dissolving it in 0.02 M NaOH. The standard sample of 2,6-dibromo-*p*-benzoquinone (2,6DBQ) was synthesized according to a previous report [32]. A natural zeolite sample was obtained from the town of Niki (Hokkaido, Japan). All other reagents were purchased from Wako Pure Chemicals (Osaka, Japan) and were used without further purification. The ultra-pure water, prepared by a Millipore ultra-pure system from distilled water, was used in all experiments.

2.2. Synthesis of Fe-Z

The cation-exchange capacities (CECs) for each sample were determined, as described in a previous report [23], and the CEC of the natural zeolite was determined to be 170 ± 7 cmol kg^{-1}, as shown in Table 1. The zeolite powder was stirred in aqueous $FeSO_4(NH_4)_2SO_4{\cdot}6H_2O$ under a N_2 atmosphere at room temperature for 72 h, in which the amount of iron was adjusted to the equivalent mole of CEC for the zeolite. After filtration of the slurry, the resulting solid was washed with distilled water and then freeze-dried. The powder was calcined at 500 °C for 8 h to obtain the Fe-loaded catalyst (Fe-Z). The inorganic element compositions (Al, Si, Ca and Fe) and specific surface areas (SSAs) for the original zeolite and Fe-Z were determined, as described in a previous report [24]. As shown in Table 1, the iron content (wt%) in the Fe-Z was 1.54 ± 0.06%, corresponding to be 276 ± 11 μmol-Fe g^{-1}. In the present study, this was considered to be moles of catalytic sites in the Fe-Z. The specific surface areas (SSAs), total pore volume and pore size were determined by a N_2-BET method using a BECKMAN COULTER SA3100-type instrument.

2.3. Assay for the reaction mixture

Test solutions, which contained TrBP (100 μM) and the RAs (0.25–10 mM) at pH 3, 5, 7 or 9, were prepared, and 30 mL aliquots of these solutions were then placed in a 100-mL Erlenmeyer flask that contained powdered Fe-Z (2.7–54.2 mg). After adding an aqueous solution of H_2O_2 (0.25–100 mM), the reaction mixture was subjected to shaking at 25 °C. During the reaction period, an 800 μL aliquot of the test solution was withdrawn and then mixed with a 400 μL of 2-propanol, followed by vigorous mixing. After centrifugation, a 20 μL aliquot of the supernatant was injected into a PU-980 type HPLC system (Japan Spectroscopic Co. Ltd.) to determine the concentration of the residual TrBP in the reaction mixture. The detailed conditions for the HPLC analysis are described in Supplementary data (Text S1). When 2-propanol was added to a mixture of TrBP and Fe-Z without H_2O_2, nearly 100% of the TrBP was recovered. However, in the absence of 2-propanol, only 2–3% of the TrBP was adsorbed to Fe-Z. Thus, the adsorption of TrBP to the Fe-Z is negligible. The concentration of Br^- in the reaction mixture was analyzed by a DX-120 type ion chromatography (Dionex).

The oxidation products, such as 2,6DBQ, that were produced in the reaction were acetylated, and these resulting acetyl derivatives were analyzed using a GC/MS system after extraction with *n*-hexane. The detailed procedures are described in Supplementary data (Text S2). The mass spectra of the detected peaks were assigned based on peaks for fragmentation ions.

In the test for TrBP mineralization, aqueous mixtures containing 5 mM NH_2OH and 100 μM TrBP at pH 3, 5, 7 or 9 were prepared, and 30 mL aliquots of these solutions were placed to the 100-mL Erlenmeyer flask that contained 13.1 mg of Fe-Z. After adding a 150 μL aliquot of 1 M aqueous H_2O_2, the flask was allowed to shake for 180 min. After the reaction, a 20 mL aliquot of the reaction mixture was mixed with 1 M aqueous Na_2SO_3 (1 mL), and the TOC of the solution was analyzed using a TOC-V CSH-type analyzer (Shimadzu).

The consumption of H_2O_2 during the reaction was monitored using a 30-mL aliquot of the reaction mixture, which contained H_2O_2 (5 mM) and Fe-Z (436 mg L^{-1} for NH_2OH and 216 mg L^{-1} for ASC) in the absence and presence of RAs (5 mM for NH_2OH and 7 mM for ASC) at pH 3 and 9. A 200-μL aliquot of the reaction mixture was withdrawn and transferred to a 1.5-mL centrifuge tube. After centrifugation, a 10 μL aliquot of the supernatant was diluted to 5 mL with pure water. The H_2O_2 in this solution was quantitatively determined by an *N*,*N*,-diethyl-*p*-phenylenediamine colorimetry [33].

The iron in the reaction mixture, eluted from the Fe-Z after a 180 min period, was analyzed by ICP-AES after filtering the reaction mixture through a membrane filter (0.45 μm).

2.4. X-ray photoelectron spectrometry

XPS spectra were recorded using a JEOL JPC-9500F-type XPS spectrometer with Mg*K*α radiation. The dried powdered sample was placed on a carbon tape attached to an aluminum sample holder. Before recording the XPS, the catalysts were evacuated in the XPS analyzer chamber. The pressure in the analysis chamber was maintained at less than 3.00×10^{-6} Pa. The analyzer was operated at a pass energy of 10 eV. The biding energy (BE) for Fe was referenced to the Si(2p) peak at 102.8 eV as an internal standard.

3. Results and discussion

3.1. Characterization of the original zeolite sample and Fe-Z

The Elemental composition, pore volume, particle size distribution, CEC and specific surface areas (SSAs), total pore volume and average pore diameter for the original zeolite and Fe-Z are summarized in Table 1. The Si/Al molar ratio of the original zeolite (15.6) remained constant compared to that for the Fe-Z (15.6). The CEC value for the Fe-Z was significantly smaller than that for the original zeolite, indicating that Fe binds tightly to the cation-exchange sites on the surface of the zeolite. The XRD patterns, shown in the Supplementary data section (Fig. S1), indicated that the minerals for the original zeolite and Fe-Z samples were clinoptilolite [(Na, K, Ca)$_4$(Si$_{30}$Al$_6$)O$_{72}$·24H$_2$O] and mordenite [(Na, K, Ca)(Si$_{10}$Al$_2$)O$_{24}$·7H$_2$O], and the structural type was consistent with the typical natural zeolite heulandite (HEU) [34]. The SSAs for the original zeolite (24.7 m^2 g^{-1}) and Fe-Z (29.2 m^2 g^{-1}) were much smaller than those for the pure zeolites (300–800 m^2 g^{-1}) [17–21], indicating that the original zeolite and Fe-Z samples contained impurities. The content of zeolite in the original zeolite and Fe-Z was estimated to be 4–10% by comparison with the reported SSAs for pure zeolites.

3.2. Influence of RAs on the kinetics of TrBP degradation

The majority of RAs can serve as HO• scavengers, leading to the inhibition of substrate oxidation via Fenton processes [35]. However, quinones have been reported to serve as electron shuttles for assisting Fe(III)/Fe(II) redox cycles in homogeneous Fenton-like processes [36], and humic acids, naturally occurring polyphenols, are also able to reduce Fe(III) [37]. In addition, oxalic acid, ASC and NH_2OH are known as strong RAs that are used for the reduction of Fe(III) [38,39]. Thus, the addition of these RAs was first examined for the degradation of TrBP via the heterogeneous Fenton-like system with the Fe-Z catalyst at pH 3.

Fig. 1 shows the degradation kinetics of TrBP in the presence and absence of RAs. In the presence of Fe-Z alone without RAs (g in Fig. 1), only 5% of the TrBP was degraded during a 180 min period, even in the presence of H_2O_2 (20 mM). For the controls without H_2O_2 and in the presence of H_2O_2 without the Fe-Z catalyst, no TrBP disappearance was observed. In Haber-Weiss processes leading to the generation of HO• by the catalytic decomposition of H_2O_2 (Eq. (1)), the Fe(III) species can be reduced to Fe(II) by H_2O_2 and HO_2•, as shown below [36]:

$$\mathrm{Fe(III) + H_2O_2 \rightarrow Fe(II) + HO_2^{\bullet} + H^+} \quad (k = 10^{-3}\text{–}10^{-2}\ \mathrm{M^{-1}\,s^{-1}}) \qquad (2)$$

$$\mathrm{Fe(III) + HO_2^{\bullet} \rightarrow Fe(II) + O_2 + H^+} \quad (k = 1 \times 10^{4}\ \mathrm{M^{-1}\,s^{-1}}) \qquad (3)$$

In the Fenton and Fenton-like processes, H_2O_2 can assist the Fe(III)/Fe(II) redox cycle, as described in Eq. (2), while the rate of this reaction is much smaller than that for the formation of HO•

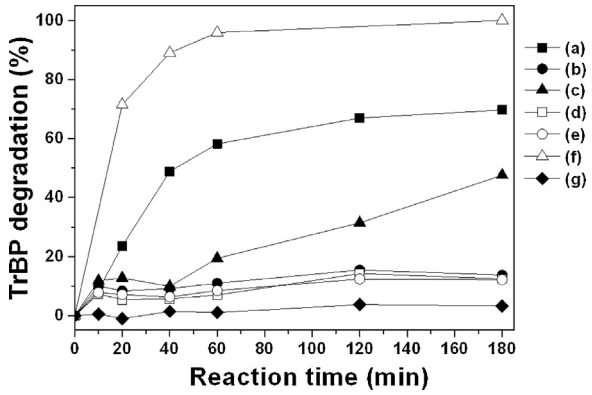

Fig. 1. Effects of reducing agents on the kinetics of TrBP degradation. (a) ASC, (b) oxalic acid, (c) *p*-hydroquinone, (d) humic acid, (e) gallic acid, (f) NH_2OH, (g) without RAs, concentrations 50 mg L^{-1} for humic acid and 10 mM for other reducing agents. [TrBP]$_0$ 100 μM, [H_2O_2] 20 mM, Fe-Z 109 mg L^{-1} (30 μM), pH 3.

via the Haber–Weiss reaction in Eq. (1). In Fig. 1, the concentration of Fe-Z (109 mg L^{-1}) was smaller than those for the reported systems (500–1000 mg L^{-1}) [16–21]. However, when the concentration of Fe-Z was increased to 873 mg L^{-1}, no enhancement in TrBP degradation was detected in the presence of catalyst alone.

To enhance the reduction of Fe(III) to Fe(II) on the surface of the Fe-Z, variety of RAs were tested, as shown in Fig. 1a–f. All of the RAs enhanced the degradation of TrBP, compared to the case in the presence of the Fe-Z alone (g in Fig. 1). Among these, ASC and NH_2OH (a and f in Fig. 1) were particularly effective RAs in terms of enhancing the degradation of TrBP. Thus, oxidation characteristics of TrBP in the heterogeneous Fenton-like system with the Fe-Z were investigated by focusing on ASC and NH_2OH.

3.3. Optimization of dosages

Fig. 2a shows the influence of RA concentration on the percent degradation of TrBP and debromination at pH 3 for a 180 min period. The percent degradation of TrBP and debromination increased with increasing RA concentrations. Although more than 90% of the TrBP and the release of 225–270 μM Br$^-$, corresponding to 2.3–2.7 bromine atoms in the degraded TrBP, were observed at concentrations of NH_2OH above 3 mM. However, in the presence of ASC, the maximum percent of TrBP degradation approached, but did not exceed 70%, and the concentration of Br$^-$ reached 120–125 μM.

The influence of H_2O_2 concentration on the degradation and debromination of TrBP were investigated in the presence of 5 mM NH_2OH and 7 mM ASC (Fig. 2b). A 95% degradation of TrBP was achieved at concentrations of H_2O_2 above 2.5 mM, although debromination increased up to 5 mM H_2O_2 and decreased thereafter. Br$^-$ is known to serve as HO• scavenger ($k < 1 \times 10^6\ \mathrm{M^{-1}\,s^{-1}}$) [5]. Thus, the slight decrease in Br$^-$ concentration at concentrations of H_2O_2 above 5 mM may be attributed to the oxidation of Br$^-$. In the presence of ASC, the percent degradation of TrBP reached a plateau of 60–65%, even when a higher concentration of H_2O_2 (100 mM) was used. Based on the experimental data shown in Fig. 2a and b, the following concentrations of RAs and H_2O_2 were determined to be optimal for the degradation of TrBP at 109 mg L^{-1} of Fe-Z: [RA] 5 mM, [H_2O_2] 5 mM for NH_2OH; [RA] 7 mM, [H_2O_2] 20 mM for ASC.

3.4. Influence of Fe-Z concentration on the reaction kinetics

Fig. 3 shows the influence of Fe-Z concentration on the kinetics of degradation and debromination of TrBP at pH 3. In the presence of NH_2OH (Fig. 3a and c), the initial rates for degradation

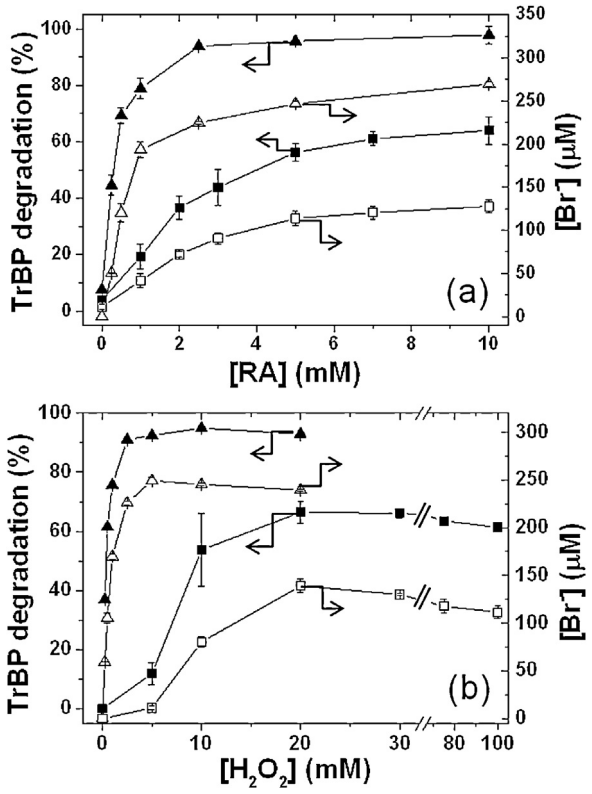

Fig. 2. Influence of the concentration of RAs (a) and H_2O_2 (b) on TrBP degradation (▲ and ■) and debromination (Δ and □). ▲ and Δ: NH_2OH, ■ and □: ASC. (a) $[TrBP]_0$ 100 μM, $[H_2O_2]$ 20 mM, Fe-Z 109 mg L^{-1} (30 μM), 180 min, pH 3; (b) $[TrBP]_0$ 100 μM, [RAs] 5 mM for NH_2OH and 7 mM for ASC, Fe-Z 109 mg L^{-1} (30 μM), 180 min, pH 3.

and debromination of TrBP increased with an increase in the catalyst concentration, while the initial rates were stagnated above 436 mg L^{-1} of Fe-Z. In the presence of ASC (Fig. 3b and d), the initial rates for degradation and debromination of TrBP also increased with an increase in the catalyst concentration, although the TrBP was not degraded and debrominated completely, even in the higher concentration of the catalyst (827 mg L^{-1}). These results suggest that, in terms of the complete degradation and debromination of TrBP, the addition of ASC is not effective, although NH_2OH is a useful RA. From the experiments of afterward, 436 mg L^{-1} of Fe-Z was selected as the catalyst concentration for the case of NH_2OH to degrade TrBP completely.

3.5. Influences of pH on the kinetics of TrBP degradation

Fig. 4 shows the influence of kinetics of degradation and debromination by a heterogeneous Fenton-like reaction with the Fe-Z in the presence of NH_2OH (a and c) or ASC (b and d). At pH 3 and 5, TrBP was completely degraded within 60 min and the complete debromination (approximately 300 μM), which corresponds to the release of 3 bromine atoms from the degraded TrBP, was observed in the presence of NH_2OH. However, the degradation and debromination of TrBP were retarded at pH 7 (Fig. 4a and c, ▲). In addition, a minor amount of degradation of TrBP and debromination were observed at pH 9 (Fig. 4a and c, ▼). Thus, the effective pH values for debromination and degradation in the presence of NH_2OH were 3 and 5.

On the other hand, the pseudo-first-order rate constants for TrBP degradation remained constant in the pH range of 3–9 in the presence of ASC (2.0×10^{-2}–2.7×10^{-2} min^{-1}, Fig. 4b and d), while these values were slightly smaller than those at pH 3 and 5 in the presence of NH_2OH (6.0×10^{-2}–6.2×10^{-2} min^{-1}). Although the efficiency of TrBP degradation and debromination were independent of solution pH in the presence of ASC, the percent degradation

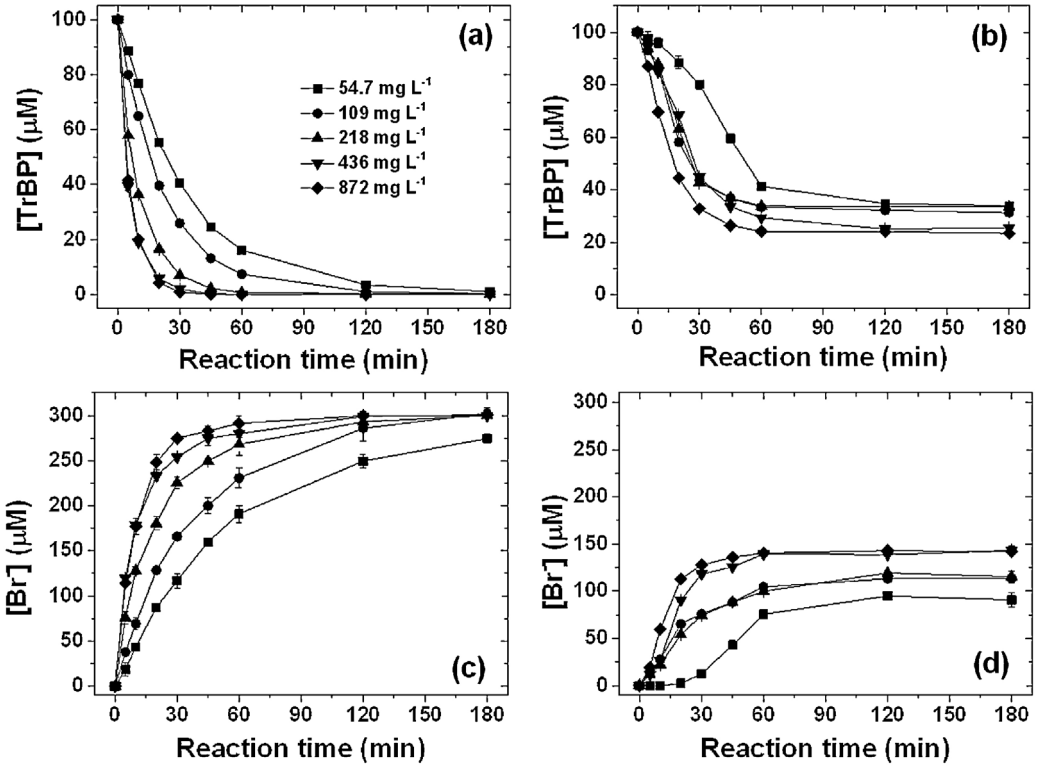

Fig. 3. Influence of the concentration of Fe-Z on the degradation and debromination of TrBP in the presence of NH_2OH (a and c) and ASC (b and d). (a) and (b) Kinetics for TrBP degradation. (c) and (d) Kinetics for debromination. (a) and (c) $[H_2O_2]$ 5 mM, $[NH_2OH]$ 5 mM, pH 3. (b) and (d) $[H_2O_2]$ 20 mM, [ASC] 7 mM, pH 3.

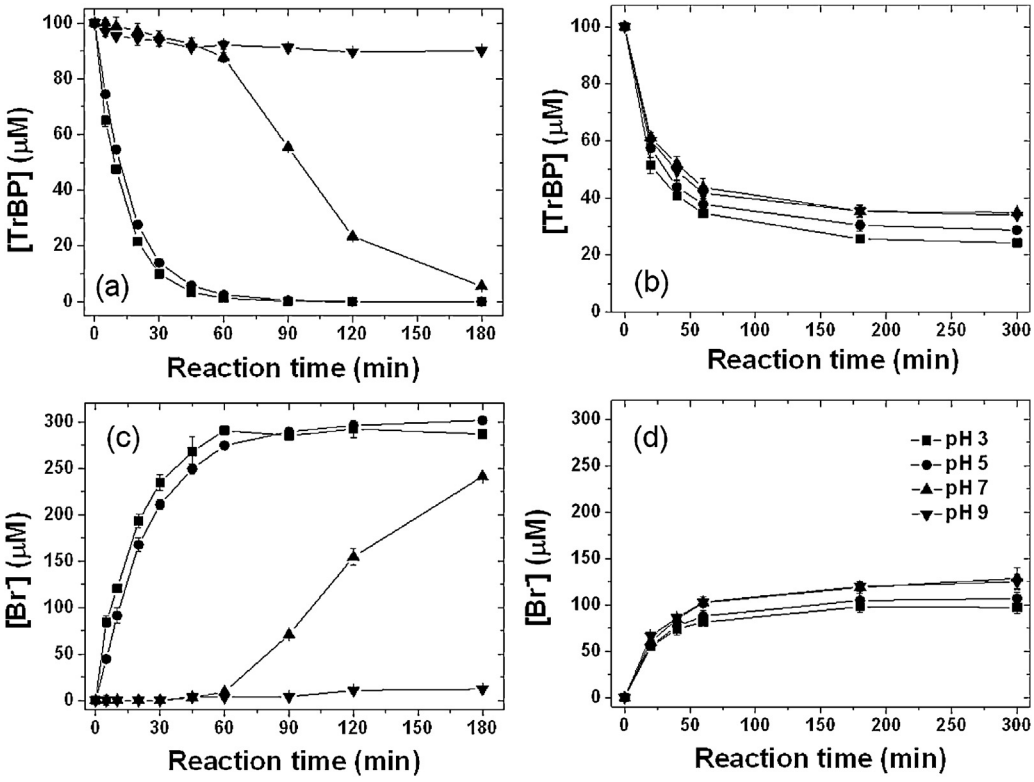

Fig. 4. Kinetic curves for the degradation and debromination of TrBP at pH 3, 5, 7 and 9. Degradation of TrBP in the presence of NH_2OH (a) and ASC (b). Debromination in the presence of NH_2OH (c) and ASC (d). $[TrBP]_0$ 100 μM, $[H_2O_2]$ 5 mM for NH_2OH and 20 mM for ASC, [RAs] 5 mM for NH_2OH and 7 mM for ASC, [Fe-Z] 436 mg L^{-1} (240 μM) for NH_2OH and 109 mg L^{-1} (60 μM) for ASC.

of TrBP and debromination reached a constant level of 65–70% and 100–120 μM, respectively. These results indicate that the complete degradation and debromination of TrBP in the presence of added ASC are difficult under any conditions (*i.e.*, concentrations of dosages and pH).

The enhanced degradation of TrBP and debromination can be attributed to the reduction of Fe(III) to Fe(II) by RAs on the Fe-Z. NH_2OH is a strong RA, when the solution pH is below its pK_a value (5.94), while the reducing power of NH_2OH is weak above pH 5.94 [28]. Thus, efficient degradation of TrBP and debromination at pH 3 and 5 (Fig. 4a and c) are due to the enhanced reduction of Fe(III) to Fe(II) by NH_2OH. At pH 7 in the presence of NH_2OH, the measured pH in the reaction mixture after a 180 min period was 3.4, while the pH in the reaction mixture at pH 9 decreased to 7.2. Thus, the retardation of TrBP degradation and debromination at pH 7 in the presence of NH_2OH (Fig. 4a and c, ▲) can be attributed to the fact that the reduction of Fe(III) to Fe(II) is initially retarded, and the attack of the generated $HO^•$ to TrBP subsequently proceeds when the pH in the reaction mixture decreases. In contrast, ASC can reduce Fe(III) to Fe(II) in a wide pH range [29]. However, the stagnation of TrBP degradation and debromination suggests that the capability for $HO^•$ scavenging by ASC is higher than that by NH_2OH.

3.6. Oxidation products and mineralization

The oxidation of bromophenols may produce a variety of brominated quinones and oligomers [32,40]. Fig. 5 shows the GC/MS chromatograms of the extracts from reaction mixtures in the presence of ASC at pH 3, 5, 7 and 9 after a 180-min period. Although no oxidation products were detected at pH 3, the diacetate derivative of 2,6-dibromo-*p*-benzoquinone (2,6DBQ, peak 1) was found as the major byproduct at pH 5, 7 and 9. Based on a standard

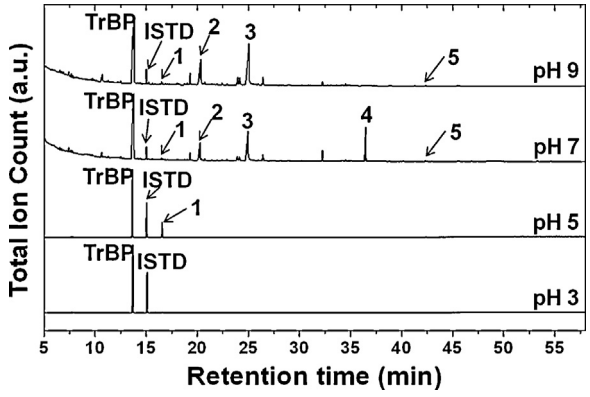

Fig. 5. The GC/MS chromatograms of a hexane extract of the reaction mixture at pH 3, 5, 7 and 9 in the presence of ASC. $[TrBP]_0$ 100 μM, $[H_2O_2]$ 20 mM, [ASC] 7 mM, Fe-Z 109 mg L^{-1} (30 μM), reaction time 180 min.

sample of 2,6DBQ, the percent conversions of the degraded TrBP into 2,6DBQ were estimated to be as follows: pH 5, 20.3%; pH 7, 11.6%; pH 9, 9.0%, decreasing with an increase in pH. Instead of peak 1, peaks 2, 3, 4 and 5 increased at pH 7 and 9. Based on their mass spectra, these peaks were assigned to specific products (Table 2). Although peak 5 was a dimer of TrBP, a more persistent compound, this amount was quite small. In contrast, no peaks corresponding to oxidation products were observed in the presence of NH_2OH at pH 3, 5, 7 and 9 after a 180 min period, suggesting the formation of the degradation of byproducts that are listed in Table 2.

As shown in Fig. 5, only 2,6DBQ was detected as a major intermediate at pH 5. Thus, the kinetic curves of 2,6DBQ formation were compared in the presence of ASC and NH_2OH at pH 5 (Fig. 6). In the presence of NH_2OH, 2,6DBQ formation rapidly increased up to a reaction time of 30 min, decreased thereafter and then disappeared

Table 2
Mass spectral assignments for oxidation products corresponding to peaks 1–5 in Fig. 4.

Peak No.	*m/z* [rel. int., fragment identity]	Assigned structures
1	325 [1.02, M^+], 310 [7.75, $(M-CH_2CO)^+$], 268 [34.15, $(M-2CH_2CO)^+$]	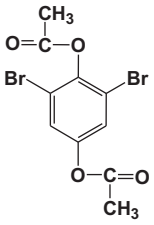
2	430 [1.24, M^+], 388 [4.46, $(M-CH_2CO)^+$], 346 [30.47, $(M-2CH_2CO)^+$]	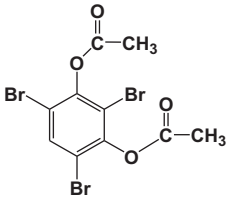
3	410 [1.44, M^+], 368 [3.57, $(M-CH_2CO)^+$], 326 [12.67, $(M-2CH_2CO)^+$], 284 [17.29, $(M-3CH_2CO)^+$]	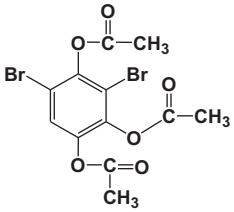
4	450 [1.52, M^+], 408 [9.22, $(M-CH_2CO)^+$], 366 [33.52, $(M-2CH_2CO)^+$], 349 [30.32, $(M-(CH_2CO)_2OH)^+$]	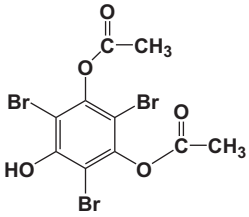
5	586 [8.18, M^+], 544 [29.53, $(M-CH_2CO)^+$], 527 [16.36, $(M-OCOCH_3)^+$], 505 [2.06, M−HBr], 293 [2.07, $C_6H_2OBr_2CH_2CO)^+$]	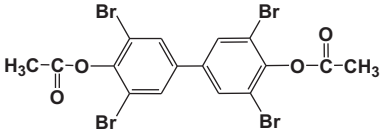

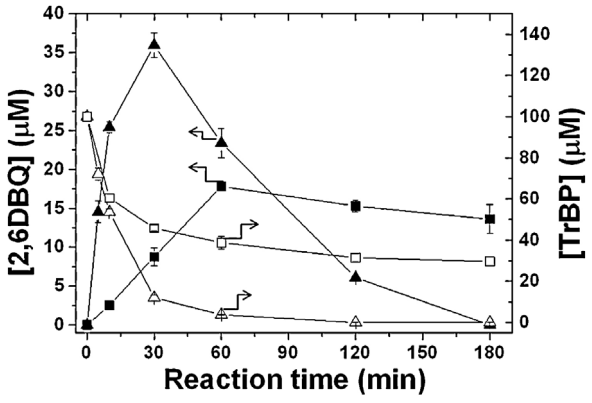

Fig. 6. Kinetics of TrBP degradation and 2,6DBQ formation at pH 5 in the presence of NH_2OH (▲ and △) or ASC (■ and □). $[TrBP]_0$ 100 μM, $[H_2O_2]$ 5 mM for NH_2OH and 20 mM for ASC, [RAs] 5 mM for NH_2OH and 7 mM for ASC, [Fe-Z] 436 mg L^{-1} (240 μM) for NH_2OH and 109 mg L^{-1} (60 μM) for ASC.

after a 180 min period. In the presence of ASC, the 2,6DBQ concentration increased up to 60 min and then gradually decreased up to 180 min, suggesting that the degradation of 2,6DBQ was incomplete.

It is known that *p*-benzoquinone can be mineralized via oxidative ring-cleavage [26]. Thus, the disappearance of 2,6DBQ may be related to its mineralization. Fig. 7a shows the percent mineralization of TrBP and the numbers of bromine atoms released from TrBP during the oxidation reaction at pH 3, 5, 7 and 9 in the presence of NH_2OH after a 180 min period. The percent mineralization decreased with an increase in pH, and no mineralization was observed at pH 9.

For practical use, the degradation in the neutral to weak acid region is preferable. The percents mineralization at pH 5 and 7 were 46% and 23%, respectively, and 0.6–0.7% of Fe was eluted from the Fe-Z at pH 5 in the presence of ASC and NH_2OH after a 180 min period. In addition, the catalytic activity for TrBP degradation was maintained after the ten recyclings of Fe-Z, as shown in Supplementary data (Fig. S2). Due to fact the trace amounts of Fe are eluted and the stability of Fe-Z, the sequential addition of NH_2OH and H_2O_2 may be useful method. To achieve the complete mineralization of TrBP, the sequential addition of H_2O_2 and NH_2OH

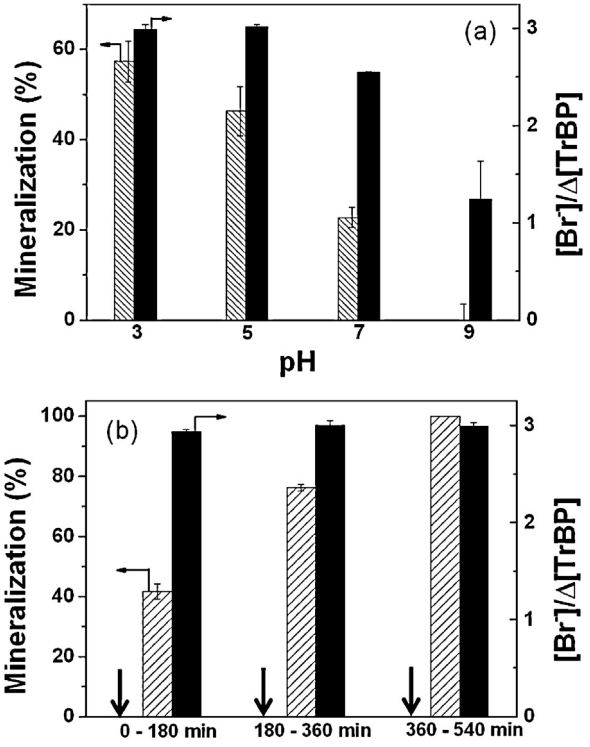

Fig. 7. Influence of pH on the percent mineralization and numbers of bromine atoms released from TrBP after a 180 min period (a), and the variations in the percent mineralization at pH 5 by the sequential addition of H_2O_2 and NH_2OH for every 180 min (b). $[TrBP]_0$ 100 μM, $[H_2O_2]$ 5 mM, $[NH_2OH]$ 5 mM, [Fe-Z] 436 mg L^{-1} (240 μM).

(5 mM) at 180 min intervals was examined (↓ in Fig. 7b). Complete mineralization was achieved after 3 additions of H_2O_2 and NH_2OH.

3.7. H_2O_2 consumption

NH_2OH and ASC reduces the Fe(III) on the Fe-Z to produce Fe(II), and H_2O_2 is decomposed by the Fe(II) to produce HO•, as shown in Eq. (1). However, NH_2OH and ASC can also serve as the HO• scavengers as follows:

$$NH_2OH + HO^\bullet \rightarrow NH_2O^\bullet + H_2O(k \leq 5 \times 10^8\ M^{-1}\ s^{-1} \text{atpH4[41]}) \quad (4)$$

$$HASC^- + HO^\bullet \rightarrow ASC^{\bullet -} + H_2O(k = 1.0 \times 10^{10}\ M^{-1}\ s^{-1}[5]) \quad (5)$$

In addition, H_2O_2 is regenerated by the disproportionation of HO• and $HO_2^\bullet$ as follows:

$$2HO^\bullet \rightarrow H_2O_2(k = 5.5 \times 10^9\ M^{-1}\ s^{-1}[5]) \quad (6)$$

$$2HO_2^\bullet \rightarrow H_2O_2 + O_2(k = 8.5 \times 10^5\ M^{-1}\ s^{-1}[36]) \quad (7)$$

$$HO_2^\bullet \leftrightharpoons H^+ + O_2^{\bullet -}(pK_a = 4.8[36]) \quad (8)$$

Although the formation of $HO_2^\bullet$ by the reduction of Fe(III) with H_2O_2 (Eq. (2)) is very slow, the disproportionation of the generated HO• (Eq. (6)) is fast reaction. Thus, the generated HO• may be recombined to form H_2O_2, if no scavengers are present. However, H_2O_2 and Fe(II) in the system can serve as HO• scavengers as follows:

$$H_2O_2 + HO^\bullet \rightarrow HO_2^\bullet + H_2O(k = 2.7 \times 10^7\ M^{-1}\ s^{-1}[5]) \quad (9)$$

$$Fe^{2+} + HO^\bullet \rightarrow FeOH^{2+}(k = 4.3 \times 10^8\ M^{-1}\ s^{-1}[5]) \quad (10)$$

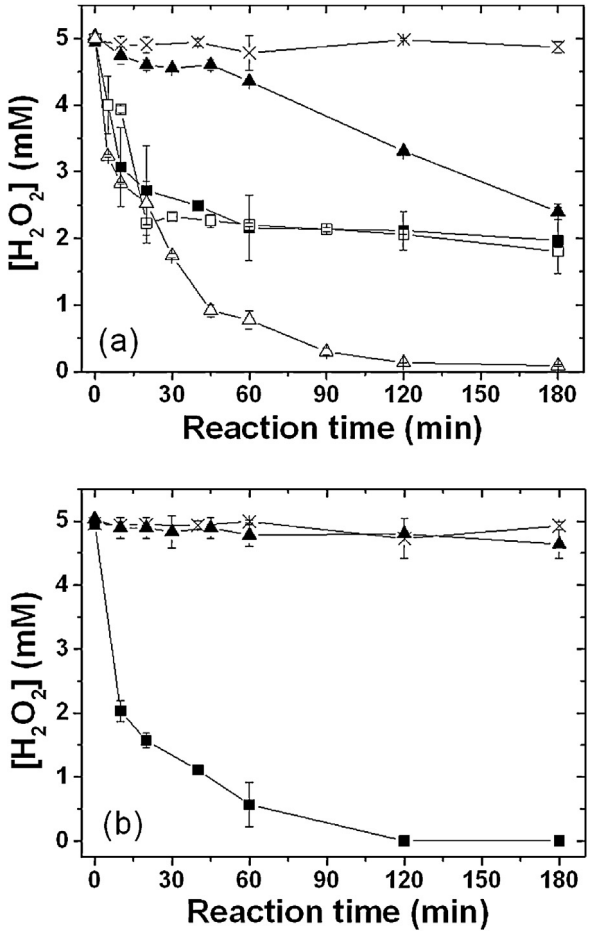

Fig. 8. Kinetics of H_2O_2 decomposition at pH 3 (a) and 9 (b). Without RAs (×), NH_2OH alone (▲), ASC alone (■), NH_2OH + TrBP (Δ) and ASC + TrBP (□). $[TrBP]_0$ 100 μM, $[H_2O_2]$ 5 mM for NH_2OH and 20 mM for ASC, [RAs] 5 mM for NH_2OH and 7 mM for ASC, [Fe-Z] 436 mg L^{-1} (240 μM) for NH_2OH and 109 mg L^{-1} (60 μM) for ASC.

Reactions (1), (2) and (9) are related to the consumption of H_2O_2. Because the concentration of H_2O_2 was much larger than those of Fe(II) and HO•, Eq. (9) would be dominant reaction for H_2O_2 consumption in the absence of RAs and TrBP. The levels of remained H_2O_2 in the reaction mixture can be determined by the balance between consumption and recombination. The consumption of H_2O_2 may be enhanced in the presence of RAs and TrBP, because HO• recombination in Eq. (6) is suppressed. To verify this, the kinetics of H_2O_2 consumption were examined in the absence and presence of RAs and TrBP.

Fig. 8 shows the consumption of H_2O_2 at pH 3 and 9 in the presence of ASC and NH_2OH. Even in the absence of TrBP (▲ and ■), H_2O_2 underwent decomposition at pH 3, compared to that in the presence of Fe-Z alone (Fig. 8a, ×). H_2O_2 was largely consumed at pH 9 in the presence of ASC, while no H_2O_2 decomposition was observed for the case of NH_2OH (Fig. 8b, ▲). At pH 3 in the presence of NH_2OH alone (Fig. 8a, ▲), a slight decomposition of H_2O_2 was observed up to 60 min, while decomposition was enhanced thereafter. The small decrease in H_2O_2 concentration is due to the scavenging of HO• by H_2O_2 and Fe(II), and the increased Fe(II) may mainly serves as a HO• scavenger after 60 min. The fact that no decomposition of H_2O_2 occurred at pH 9 in the presence of NH_2OH alone (Fig. 8b, ▲) can be attributed to the fact that Fe(III) is not reduced to Fe(II) in weakly alkaline pH [28]. The larger decomposition rate of H_2O_2 in the presence of ASC at pH 3 and 9 (Fig. 8, ■) demonstrates the capability of ASC for scavenging HO•, which is much larger than that for NH_2OH, consistent with Eqs. (4) and (5).

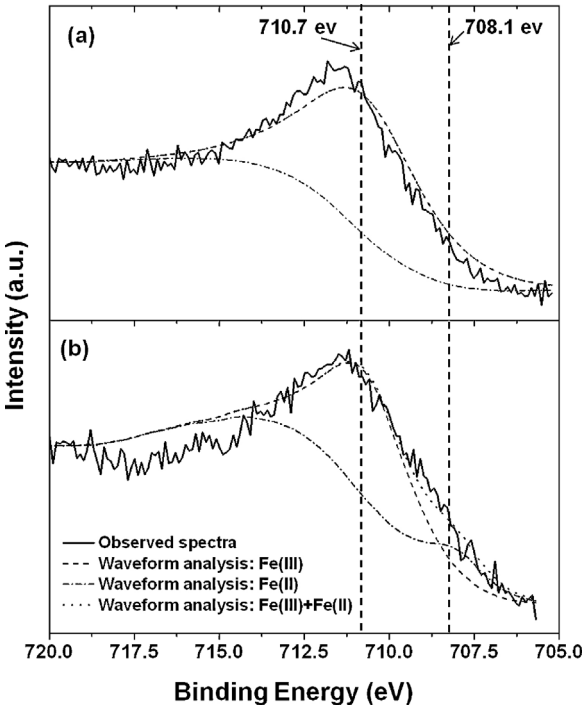

Fig. 9. Fe(2p)$_{3/2}$ core-level XPS spectrum of the Fe-Z before (a) and after treatment with ASC (b). Conditions for the treatment: pH 9; ASC 10 mM; Fe-Z 200 mg L^{-1}; reaction time, 180 min.

When the TrBP was added to the reaction mixture at pH 3 in the presence of NH_2OH, the H_2O_2 rapidly decomposed (Fig. 8a, Δ), compared to the kinetic curve without TrBP (Fig. 8a, ▲). In contrast, the kinetics in the presence of ASC (Fig. 8a, ■ and □) were unchanged, even when TrBP was added. These results indicate that the efficiency of NH_2OH for scavenging HO• is much lower than that of TrBP and the oxidation of TrBP is the dominant reaction in the presence of NH_2OH.

3.8. Analysis of Fe on the Fe-Z by XPS

To elucidate the effect of RAs on the enhancement in Fenton degradation, the states of Fe(III) on the surface of the Fe-Z were compared before and after treating with ASC. The ASC-treated Fe-Z was readily oxidized to Fe(III) under aerobic conditions. Thus, after treating the Fe-Z with the ASC, the sample was immediately transferred to a vacuum desiccator and dried *in vacuo*. The sample was stored in the desiccators until XPS spectra were obtained. Fig. 9 shows the Fe(2p)$_{3/2}$ core-level XPS spectra for Fe-Z before (a) and after treatment with ASC (b). The BEs for Fe(III) and Fe(II) species appear at 710.7 eV and 708.1 eV, respectively, based on those for magnetite (Fe_3O_4), which is a mixture of Fe(III) and Fe(II). The peak components for Fe(III) and Fe(II) in Fe-zeolite are close to one another (711.6–712.5 eV for Fe(III) and 709.9–710.4 eV for Fe(II)) [42]. Thus, waveform analyses were carried out for the Fe(2P)$_{3/2}$ peaks. The rates of Fe(III) and Fe(II) components before and after treatment with ASC were estimated as follows: before the reaction, 100% Fe(III), 0% Fe(II); after ASC treatment, 82% Fe(III), 18% Fe(II). These values confirm that RAs such as ASC can assist the Fe(III)/Fe(II) redox cycle to enhance the generation of HO•.

3.9. Significance in application

Adding NH_2OH to a heterogeneous Fenton-like system with the Fe-Z was more advantageous than the addition of ASC, in terms of the complete mineralization of TrBP. For the case of NH_2OH, the end products of the reduction of Fe(III) are N_2, N_2O, NO_3^- and NO_2^- [28]. At pH 3 and 5, approximately 30% of the NH_2OH was converted into NO_3^- and NO_2^- after a 180 min reaction period, as shown in Supplementary data (Fig. S3). However, the formation of NO_3^- and NO_2^- is not desirable, and they should be removed before being sent to an aquatic environment by combining this process with an additional treatment technique (e.g., microbial treatment [42]). NH_2OH is commercially available as a 50% (*ca.* 15 M) aqueous solution (CAS No. 7803-49-8). As shown in Fig. 6b, three additions of 5 mM NH_2OH is required to completely mineralize TrBP. Approximately 1 L of a 50% aqueous NH_2OH is required for the treatment of 1 m^3 of wastewater. This may be a reasonable amount and suggests that such a system might be applicable for the treatment of wastewater.

4. Conclusions

Fe(II) was loaded onto the cation-exchange sites in a natural zeolite, and was strongly bound as the Fe(III) ionic form after calcination at 773 K. Although the prepared Fe-Z was not effective for the oxidation of TrBP via a Fenton-like process, the addition of ASC or NH_2OH resulted in a significant enhancement in the degradation and debromination of TrBP. The kinetics of TrBP degradation and H_2O_2 consumption indicate that ASC serves as a strong HO• scavenger at any pH and leads to the incomplete degradation of TrBP. Thus, ASC was not an effective RA for the enhanced degradation and debromination of TrBP. In contrast, the complete degradation and debromination of TrBP could be achieved at pH 3 and 5 in the presence of NH_2OH, indicating that this RA is a suitable additive for enhancing heterogeneous Fenton-like oxidation reactions using Fe-Z. In addition, TrBP was completely mineralized at pH 5 after the sequential addition of H_2O_2 and NH_2OH. The role of RAs are to enhance the reduction of Fe(III) on the Fe-Z to Fe(II), which permits the generation of HO• to be accelerated via the Haber Weiss reaction.

Acknowledgment

This work was supported by Grants-in-Aid for Scientific Research from Japan Society for Promotion of Science (25241017).

Appendix A. Supplementary data

Supplementary data associated with this article can be found, in the online version, at http://dx.doi.org/10.1016/j.apcatb.2013.09.032.

References

[1] W.-J. Sim, S.-H. Lee, I.-S. Lee, S.-D. Choi, J.-E. Oh, Chemosphere 77 (2009) 552–558.
[2] I.A.T.M. Meerts, J.J. Zanden, E.A.C. Luijuks, I. van Leeuwen-Bol, G. Marsh, E. Jakobsson, A. Bergman, A. Brouwer, Toxicol. Sci. 56 (2000) 95–104.
[3] M. Fukushima, Y. Mizutani, S. Maeno, Q. Zhu, H. Kuramitz, S. Nagao, Molecules 17 (2012) 48–60.
[4] F. Haber, J. Weiss, Naturwissenschaften 20 (1932) 948–950.
[5] G.V. Buxton, C.L. Greenstock, W.P. Helman, A.B. Ross, J. Phys. Chem. Ref. Data 17 (1988) 513–886.
[6] M. Pera-Titus, V. García-Molina, M.A. Baños, J. Giménez, S. Esplugas, Appl. Catal. B: Environ. 47 (2004) 219–256.
[7] M. Fukushima, K. Tatsumi, Environ. Sci. Technol. 35 (2001) 1771–1778.
[8] M. Fukushima, K. Tatsumi, K. Morimoto, Environ. Toxicol. Chem. 19 (2000) 1711–1716.
[9] M.A. Tarr (Ed.), Chemical Degradation Methods for Wastes and Pollutants – Environmental and Industrial Applications, Dekker, New York, 2003, pp. 165–200.
[10] L. Xu, J. Wang, Appl. Catal. B: Environ. 123–124 (2012) 117–126.
[11] J.H. Ramirez, C.A. Costa, L.M. Madeira, G. Mata, M.A. Vicente, M.L. Rojas-Cervantes, A.J. López-Peinado, R.M. Martín-Aranda, Appl. Catal. B: Environ. 71 (2007) 44–56.

[12] M.N. Timofeeva, S.T. Khankhasaeva, Y.A. Chesalov, S.V. Tsybulya, V.N. Panchenko, E.T. Dashinamzhilova, Appl. Catal. B: Environ. 88 (2009) 127–134.
[13] J. Herney-Ramirez, M.A. Vicente, L.M. Madeira, Appl. Catal. B: Environ. 98 (2010) 10–26.
[14] R.-M. Liou, S.-H. Chen, M.-Y. Hung, C.S. Hsu, Chemosphere 55 (2004) 1271–1280.
[15] R.-M. Liou, S.-H. Chen, M.-Y. Hung, C.S. Hsu, J.-Y. Lai, Chemosphere 59 (2005) 117–125.
[16] S. Navalon, M. Alvaro, H. Garcia, Appl. Catal. B: Environ. 99 (2010) 1–26.
[17] M. Neamţu, C. Zaharia, C. Catrinescu, A. Yediler, M. Macoveanu, A. Kettrup, Appl. Catal. B: Environ. 48 (2004) 287–294.
[18] M. Neamţu, C. Catrinescu, A. Kettrup, Appl. Catal. B: Environ. 51 (2004) 149–157.
[19] W. Najjar, S. Azabou, S. Sayadi, A. Ghorbed, Appl. Catal. B: Environ. 88 (2009) 299–304.
[20] R. Gonzalez-Olmos, M. Martin, A. Georgi, F.-D. Kopinke, I. Oller, Appl. Catal. B: Environ. 125 (2012) 51–58.
[21] R. Gonzalez-Olmos, F. Holzer, F.-D. Kopinke, A. Georgi, Appl. Catal. A: Gen. 398 (2011) 44–53.
[22] S. Wang, Z.H. Zhu, J. Hazard. Mater. B318 (2006) 946–952.
[23] A. Miura, R. Okabe, K. Izumo, M. Fukushima, Appl. Clay Sci. 46 (2009) 277–282.
[24] S. Fukuchi, A. Miura, R. Okabe, M. Fukushima, M. Sasaki, T. Sato, J. Mol. Struct. 982 (2010) 181–186.
[25] S. Fukuchi, M. Fukushima, R. Nishimoto, G. Qi, T. Sato, Clay Miner. 47 (2012) 355–364.
[26] M. Fukushima, K. Tatsumi, K. Morimoto, Environ. Sci. Technol. 34 (2000) 2006–2013.
[27] C.A. Martínez-huitle, E. Brillas, Appl. Catal. B: Environ. 87 (2009) 105–145.
[28] L. Chen, J. Ma, X. Li, J. Zhang, J. Fang, Y. Guan, P. Xie, Environ. Sci. Technol. 45 (2011) 3925–3930.
[29] Y. Li, T. Zhu, J. Zhao, B. Xu, Environ. Sci. Technol. 46 (2012) 10304–10309.
[30] M. Fukushima, M. Kawasaki, A. Sawada, H. Ichikawa, K. Morimoto, K. Tatsumi, S. Tanaka, J. Mol. Catal. A: Chem. 187 (2002) 201–213.
[31] M. Fukushima, S. Tanaka, K. Nakayasu, K. Sasaki, K. Tatsumi, Anal. Sci. 15 (1999) 185–188.
[32] S. Shigetatsu, M. Fukushima, S. Nagao, J. Environ. Sci. Health A 45 (2010) 1536–1542.
[33] M. Fukushima, K. Tatsumi, Talanta 47 (1998) 899–905.
[34] K. Elaiopoulos, Th. Perraki, E. Grigoropoulou, Microporous Mesoporous Mater 112 (2008) 441–449;
R.J. Reiter, D.-X. Tan, L.C. Manchester, W. Qi, Cell Biochem. Biophys. 34 (2001) 237–256.
[35] R. Chen, J.J. Pignatello, Environ. Sci. Technol. 31 (1997) 2399–2406.
[36] M. Fukushima, K. Tatsumi, Colloid Surf. A: Physicochem. Eng. Asp. 155 (1999) 249–258.
[37] Y. Zuo, J. Hoigné, Environ. Sci. Technol. 26 (1992) 1014–1022.
[38] H. Iwai, M. Fukushima, M. Yamamoto, Anal. Sci. 29 (2013) 723–728.
[39] M. Fukushima, Y. Ishida, S. Shigematsu, H. Kuramitz, S. Nagao, Chemosphere 80 (2010) 860–865.
[40] M. Simic, E. Hayon, J. Am. Chem. Soc. 93 (1971) 5982–5986.
[41] J. Duxiao, H. Nongyue, Z. Yuanying, X. Chunxiang, Y. Chunwei, L. Zuhong, Mater. Chem. Phys. 69 (2001) 246–251.
[42] Z. Shen, Y. Zhou, J. Wang, Bioresour. Technol. 131 (2013) 33–39.